IEICE Proceeding Series

Detection of coupling directions with intersystem recurrence networks

Norbert Marwan, Jan H. Feldhoff, Reik V. Donner, Jonathan F. Donges, Jürgen Kurths

Vol. 1 pp. 231-234
Publication Date: 2014/03/17
Online ISSN: 2188-5079

2012 International Symposium on Nonlinear Theory and its Applications
NOLTA2012, Palma, Majorca, Spain, October 22-26, 2012

Detection of coupling directions with intersystem recurrence networks

Norbert Marwan†, Jan H. Feldhoff†‡, Reik V. Donner†, Jonathan F. Donges†‡, Jürgen Kurths†‡

†Potsdam Institute for Climate Impact Research, 14412 Potsdam, Germany
‡Institute of Physics, Humboldt Universität zu Berlin, Newtonstr. 15, 12489 Berlin, Germany
Email: marwan@pik-potsdam.de

Abstract—We describe and apply a novel concept for inferring coupling directions between dynamical systems based on geometric properties in phase space reconstructed from time series. The approach combines the recently introduced techniques for (1) studying interacting networks and (2) construction of complex networks from time series by their recurrence structure: we extend the approach of cross-recurrence between two systems towards an intersystem recurrence network and apply measures for studying interacting networks on it. These measures allow us to examine the emergence of typical geometric signatures in the driven relative to those of the driving system and vice versa, and, therefore, reveal signs of coupling directions. We demonstrate this concept by investigating the coupling between parts of the Asian monsoon system as seen from a palaeo-climate perspective.

1. Introduction

The study of causal dependencies is one of the most important fields in complex systems theory. Available approaches range from using linear models [1], information based methods [2], synchronisation [3], to recurrence based approaches [4], to name a few. Here we propose a novel approach investigating the structures in a shared phase space of interacting dynamical systems by means of intersystem recurrence networks [5].

2. Recurrence Plots

Recurrence plots can been used as an approach for analysing time series from dynamical systems by means of graph-theoretical concepts [6–8]. It has been shown that their structural properties are closely related to the geometry of the underlying attractor and, hence, the resulting system's dynamics. A recurrence plot renders close states in a phase space, which represents the phase space dynamics and can be constructed from a measured time series if the system variables are not available [9]:

$$R_{ij}(\varepsilon) = \Theta(\varepsilon - d(x_i, x_j)), \tag{1}$$

where $d(\cdot,\cdot)$ measures some distance (e.g., according to the Euclidean or maximum norm) in phase space. The visualisation of this symmetric matrix is the *recurrence plot*, and the emergence of line structures in these recurrence plots has been intensively utilised for characterising the dynamical properties of the underlying time series by estimates of dynamical invariants and novel measures of complexity (*recurrence quantification analysis, RQA*) [9, 10].

For a complex network analysis the recurrence plot of a time series can be re-interpreted as the connectivity pattern of an associated complex network represented by an undirected simple graph [7]. Specifically, given the definition in Eq. (1) based on ε-recurrences, we can formally write $A_{ij}(\varepsilon) = R_{ij}(\varepsilon) - \delta_{ij}$ (where δ_{ij} is Kronecker's delta) to obtain the adjacency matrix of the corresponding ε-recurrence network (RN). The properties of such networks have been widely studied [8, 11–13], and their practical use as an exploratory tool of time series analysis has been demonstrated [7, 14].

Among others, one important measure of complexity derived from a recurrence network is the clustering coefficient [13, 15]

$$C_v = \frac{2}{k_v(k_v-1)} N_v^{\Delta}, \tag{2}$$

where k_v is the degree centrality (i.e., the number of neighbors of v, which coincides with the local recurrence rate RR_v), and N_v^{Δ} is the total number of closed triangular subgraphs including v, which is normalized by the maximum possible value $k_v(k_v-1)/2$. C_v corresponds to the probability that two randomly chosen neighbors of v are also neighbors. From the viewpoint of recurrences in phase space, C_v is related to the effective dimensionality of the set of observations in the ε-neighborhood of a state v [12]. It is a powerful measure for the classification of periodic and chaotic behavior in parameter space and, hence, for the identification of complex periodic windows [13].

3. Intersystem recurrence networks

Recurrence plots have been extended to cross-recurrence plots in order to study recurrences in a shared phase space [16]:

$$CR_{ij}^{XY}(\varepsilon) = \Theta(\varepsilon - d(x_i, y_j)), \tag{3}$$

with $\vec{x}_i$ and $\vec{y}_i$ the phase space trajectories of two systems X and Y. Cross-recurrence plots have been used to study interrelationships between possibly coupled dynamical systems [10, 16].

Similar to the definition of recurrence networks, we can use the cross-recurrence plot to define an intersystem re-

currence network (IRN):

$$\mathbf{IR}(\boldsymbol{\varepsilon}) = \begin{pmatrix} \mathbf{R}^X(\varepsilon_x) & \mathbf{CR}^{XY}(\varepsilon_{XY}) \\ \mathbf{CR}^{YX}(\varepsilon_{YX}) & \mathbf{R}^Y(\varepsilon_Y) \end{pmatrix} \quad (4)$$

with $\mathbf{CR}^{XY}$ being the cross-recurrence matrix between the systems X and Y and $\mathbf{R}^X = \mathbf{CR}^{XX}$ the recurrence matrix of system X (and analogous for system Y). In some cases it might be necessary to consider different recurrence thresholds [11] for the individual blocks $\mathbf{CR}^{XY}$ of the intersystem recurrence matrix, i.e., it is not required to have $\varepsilon_{XX} = \varepsilon_{YX} = \varepsilon_{YY}$.

The intersystem recurrence matrix, Eq. (4) combines all information from the (intra-system) recurrence plots $\mathbf{R}^{X,Y}$ and the cross-recurrence plots $\mathbf{CR}^{XY}$ and, thus, stands for a straightforward generalisation of the established concept of cross-recurrence plots. This formulation provides a generic way for studying the mutual interrelationships between sets of dynamical systems from a complex network perspective. Thus, the intersystem recurrence network (IRN) is $\mathbf{A}(\boldsymbol{\varepsilon}) = \mathbf{IR}(\boldsymbol{\varepsilon}) - \mathbb{I}_N$.

4. Network measures for IRNs

The IRN is a graph $G = (V, E)$ with the set V of vertices and set E of edges. It is separable into disjunct subsets $V_k \subseteq V$ and $E_{kl} \subseteq E$. Then E_{kk} contains the (internal) edges within the subgraph or subnetwork G_k, while E_{kl} comprises (cross-) edges connecting subnetworks G_k and G_l. The bipartite subgraphs $G_{kl} = (V_k \cup V_l, E_{kl})$ contain all vertices of the vertex subsets V_k and V_l, and the (cross-) edges E_{kl} between these two sets. Thus, the graphs G_X and G_Y correspond to the intra-system RNs constructed from the systems X and Y, whereas G_{XY} contain the cross-recurrence structure in terms of the sets of cross-edges E_{XY}. In the following, we will use the letters k, l to denote subnetworks and v, w, p, q for single vertices.

We define the *cross-degree* k_v^{kl}, which gives the number of edges which connect vertex v in subgraph G_k (i.e., $v \in V_k$) to any vertex in subgraph G_l, as $k_v^{kl} = \sum_{q \in V_l} A_{vq}$ [5, 17].

The *local cross-clustering coefficient* C_v^{kl} estimates the probability that two randomly drawn neighbours of vertex $v \in V_k$ from subgraph G_l are also neighbours [5]:

$$C_v^{kl} = \frac{1}{k_v^{kl}(k_v^{kl} - 1)} \sum_{p,q \in V_l} A_{vp} A_{pq} A_{qv}. \quad (5)$$

For vertices v^* with $k_{v^*}^{kl} = 0$, we define $C_{v^*}^{kl} = 0$ in order to avoid divergencies (alternatively, one could consider C_v^{kl} as undefined for these vertices). Averaging over all vertices v, we immediately get the corresponding *global cross-clustering coefficient* C^{kl}

$$C^{kl} = \langle C_v^{kl} \rangle_{v \in V_k}. \quad (6)$$

It is important to note that the global cross-clustering coefficient is *not* invariant under the permutation $i \leftrightarrow j$, i.e., $C^{XY} \neq C^{YX}$ (Fig. 1), which is in fact the foundation of the method presented in the following.

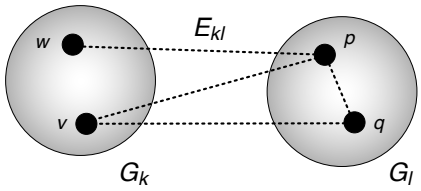

Figure 1: Two coupled subnetworks. The graph has global cross-clustering coefficients of $C^{kl} = 0.5 \neq C^{lk} = 0$.

5. Coupling directions

Let X and Y be two dynamical systems, allowing for the construction of an IRN, the structure of which can be quantified by the global cross-clustering coefficient C^{XY} and C^{YX}.

In the *uncoupled* case, C^{XY} and C^{YX} will randomly arise from the invariant densities of X and Y without any additional structural component. Therefore, we expect $C^{XY} = C^{YX}$ (Tab. 1).

For *unidirectional* coupling of the type $\dot{y} \propto f(x - y)$, where f is a monotonic function of either positive or negative sign (for example, in the case of diffusive coupling, $f(x-y) = \mu_{XY}(x-y)$, with μ_{XY} being the coupling strength). If the coupling direction is $X \to Y$ and the coupling is large enough, we are likely to also find a state y_k^* in Y, which is (cross-)recurrent to both x_i and x_j, due to the coupling's diffusive nature and thus the tendency to "drag" the trajectory of Y towards X. The resulting "cross-triangle" adds to the value of C^{YX} according to their definition. On the other hand, "cross-triangles" constituted by two recurrent states in Y and one cross-recurrent state in X are merely coincidental due to the driver-response-like coupling. We would thus expect to see $C^{YX} > C^{XY}$ in case of a unidirectional coupling $X \to Y$ and vice versa for the opposite coupling direction (Tab. 1).

For a *symmetric bidirectional* coupling, the mutual effects on both systems are equal and thus lead to IRN measures of the same magnitude. The same observation should hold if the subsystems become synchronised (at least in a generalised sense), e.g., in case of a sufficiently strong coupling (Tab. 1).

Table 1: Qualitative behaviour of cross-clustering coefficient in different coupling situations.

Coupling direction	Expected relation
no coupling	$C^{XY} \approx C^{YX}$
$X \to Y$	$C^{XY} < C^{YX}$
$Y \to X$	$C^{XY} > C^{YX}$
$X \leftrightarrow Y$	$C^{XY} \approx C^{YX}$

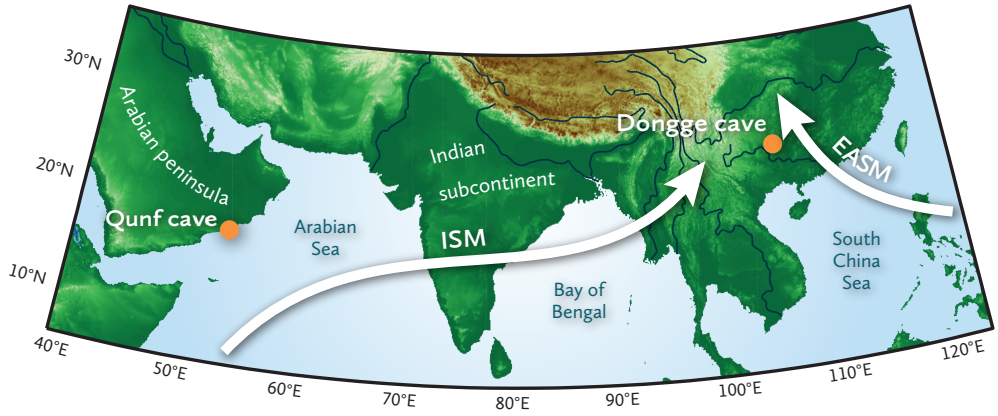

Figure 2: Main wind directions of the Indian (ISM) and East-Asian Summer Monsoon (EASM) and locations of the Qunf and Dongge caves [5].

6. Real-world example: Palaeo-climate variation

In order to demonstrate the potential of the proposed method we consider the coupling between the East Asian Summer Monsoon (EASM) and the Indian Summer Monsoon (ISM) as it performed in the last about 10,000 years (Holocene). The Asian monsoon system is not only one of the most important atmospheric circulation systems, it also has a strong socio-economic impact because it affects a major part of the world's population [18].

The ISM and EASM transport moisture from different sources to the continent (Fig. 2). Variations in oxygen isotope ratios δ^{18}O) measured in speleothems provide high-resolution proxies for the monsoon activity in the past [19, 20]. We use the variability of δ^{18}O obtained from the Dongge cave in Southeast China [19] and the Qunf cave in Oman [20] (Fig. 2). The Dongge record D represents the Holocene monsoon variation in the recent EASM region and the Qunf record Q the monsoon variation in the ISM region (Tab. 2).

Table 2: Time interval T (BP = years before 1950), mean sampling time Δt, number of observations N, and corresponding reference of the studied climate proxies.

Record	T (yr BP)	Δt (yr)	N	Ref.
Dongge D	−50...8880	4.2	2,124	[19]
Qunf Q	378...10,300	7.1	1,405	[20]

Both D and Q were detrended by a 100-yr moving-average filter. For the reconstruction of the phase space we use time-delay embedding with an embedding dimension of $d = 3$ in both cases but different time delays of $\tau_D = 3$ for the Dongge record and $\tau_Q = 2$ for the Qunf record (according to the results of the false nearest neighbors and auto-mutual information methods [21]). The different time delays account for their different average sampling rates, leading to $\tau \approx 13$ years on average for both records to make the considered state vectors actually comparable (cf. Tab. 2). From the embedded state vectors we bootstrap 80% of the data and calculate the resulting IRNs and their global cross-clustering coefficients, with $RR_D = RR_Q = 0.03$ and $RR_{DQ} = RR_{QD} = 0.02$. This procedure is carried out $M = 10,000$ times to evaluate the robustness of our results.

Figure 3 reveals that the distributions of the global cross-clustering coefficients are clearly separated by $C^{DQ} > C^{QD}$. From these results we infer that the coupling direction was $Q \to D$ during the Holocene, i.e., under the assumption that Q represents the ISM activity and D the EASM activity we find that the monsoon impact at the location of the Chinese cave was not only controlled by the EASM but also by the ISM, where the EASM did not have a comparably strong impact on the location of the Oman cave.

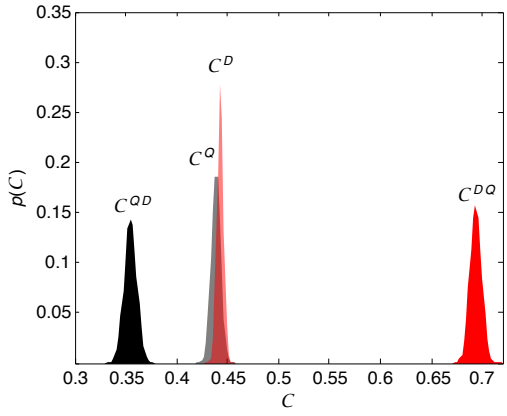

Figure 3: Normalised distributions of the global cross-clustering coefficient inferred from the Dongge and Qunf data by bootstrapping 80% of the data in $M = 10,000$ realisations. The distributions of the intersystem measures are clearly seperated with $C^{DQ} > C^{QD}$, indicating a possible coupling direction $Q \to D$.

Acknowledgments

This work was supported by the WGL project ECONS, the DFG research group HIMPAC, the IRTG 1740 (DFG/FAPESP), and the German National Academic Foundation.

References

[1] C. W. J. Granger. Investigating causal relations by econometric models and cross-spectral methods. *Econometr.*, 37(3):424–438, 1969.

[2] S. Frenzel and B. Pompe. Partial Mutual Information for Coupling Analysis of Multivariate Time Series. *Phys. Rev. Lett.*, 99:204101, 2007.

[3] A. Pikovsky, M. Rosenblum, and J. Kurths. *Synchronization – A Universal Concept in Nonlinear Sciences*. Cambridge University Press, 2001.

[4] M. C. Romano, M. Thiel, J. Kurths, and C. Grebogi. Estimation of the direction of the coupling by conditional probabilities of recurrence. *Phys. Rev. E*, 76:036211, 2007.

[5] J. H. Feldhoff, R. V. Donner, J. F. Donges, N. Marwan, and J. Kurths. Geometric detection of coupling directions by means of inter-system recurrence networks. *Phys. Lett. A*, subm.

[6] J. Zhang and M. Small. Complex network from pseudoperiodic time series: Topology versus dynamics. *Phys. Rev. Lett.*, 96(23):238701, 2006. X. Xu, J. Zhang, and M. Small. Superfamily phenomena and motifs of networks induced from time series. *Proc. Nat. Acad. Sc.*, 105(50):19601–19605, 2008. R. V. Donner, M. Small, J. F. Donges, N. Marwan, Y. Zou, R. Xiang, and J. Kurths. Recurrence-based time series analysis by means of complex network methods. *Int. J. Bif. Chaos*, 21(4):1019–1046, 2011.

[7] N. Marwan, J. F. Donges, Y. Zou, R. V. Donner, and J. Kurths. Complex network approach for recurrence analysis of time series. *Phys. Lett. A*, 373(46):4246–4254, 2009.

[8] R. V. Donner, Y. Zou, J. F. Donges, N. Marwan, and J. Kurths. Recurrence networks – A novel paradigm for nonlinear time series analysis. *New J. Phys.*, 12(3):033025, 2010.

[9] N. Marwan, M. C. Romano, M. Thiel, and J. Kurths. Recurrence Plots for the Analysis of Complex Systems. *Phys. Rep.*, 438(5–6):237–329, 2007.

[10] N. Marwan. A Historical Review of Recurrence Plots. *Europ. Phys. J. ST*, 164(1):3–12, 2008.

[11] R. V. Donner, Y. Zou, J. F. Donges, N. Marwan, and J. Kurths. Ambiguities in recurrence-based complex network representations of time series. *Phys. Rev. E*, 81:015101(R), 2010.

[12] R. V. Donner, J. Heitzig, J. F. Donges, Y. Zou, N. Marwan, and J. Kurths. The Geometry of Chaotic Dynamics – A Complex Network Perspective. *Europ. Phys. J. B*, 84:653–672, 2011.

[13] Y. Zou, R. V. Donner, J. F. Donges, N. Marwan, and J. Kurths. Identifying complex periodic windows in continuous-time dynamical systems using recurrence-based methods. *Chaos*, 20(4):043130, 2010. Y. Zou, R. V. Donner, and J. Kurths. Geometric and dynamic perspectives on phase-coherent and noncoherent chaos. *Chaos*, 22(1):013115, 2012.

[14] J. F. Donges, R. V. Donner, M. H. Trauth, N. Marwan, H. J. Schellnhuber, and J. Kurths. Nonlinear detection of paleoclimate-variability transitions possibly related to human evolution. *Proc. Nat. Acad. Sc.*, 108(51):20422–20427, 2011.

[15] D. J. Watts and S. H. Strogatz. Collective dynamics of 'small-world' networks. *Nature*, 393:440–442, 1998.

[16] N. Marwan and J. Kurths. Nonlinear analysis of bivariate data with cross recurrence plots. *Phys. Lett. A*, 302(5–6):299–307, 2002.

[17] J. F. Donges, H. C. H. Schultz, N. Marwan, Y. Zou, and J. Kurths. Investigating the topology of interacting networks. *The European Physical Journal B*, 84:635–651, 2011.

[18] Pingzhong Zhang, Hai Cheng, R Lawrence Edwards, Fahu Chen, Yongjin Wang, Xunlin Yang, Jian Liu, Ming Tan, Xianfeng Wang, Jinghua Liu, Chunlei An, Zhibo Dai, Jing Zhou, Dezhong Zhang, Jihong Jia, Liya Jin, and Kathleen R Johnson. A test of climate, sun, and culture relationships from an 1810-year Chinese cave record. *Science*, 322(5903):940–2, 2008.

[19] Yongjin Wang, Hai Cheng, R Lawrence Edwards, Yaoqi He, Xinggong Kong, Zhisheng An, Jiangying Wu, Megan J Kelly, Carolyn Dykoski, and Xiangdong Li. The Holocene Asian monsoon: links to solar changes and North Atlantic climate. *Science*, 308(5723):854–7, 2005.

[20] Dominik Fleitmann, Stephen J Burns, Manfred Mudelsee, Ulrich Neff, Jan Kramers, Augusto Mangini, and Albert Matter. Holocene forcing of the Indian monsoon recorded in a stalagmite from southern Oman. *Science*, 300(5626):1737–9, 2003.

[21] H. Kantz, T. Schreiber, and R.S. Mackay. *Nonlinear time series analysis*. Cambridge University Press, 1997.